Magnetic Anisotropy and Engineering of Magnetic Behavior of the Edges in Co Embedded Graphene Nanoribbons

Sergey Lisenkov, Antonis N. Andriotis, and Madhu Menon

Phys. Rev. Lett. **108**, 187208 — Published 4 May 2012

DOI: 10.1103/PhysRevLett.108.187208

Magnetic anisotropy and engineering of magnetic behavior of the edges in Co embedded graphene nanoribbons

Sergey Lisenkov*

Department of Physics, University of South Florida Tampa, FL 33620-5700

Antonis N. Andriotis†

Institute of Electronic Structure and Laser,

Foundation for Research and Technology-Hellas,

P.O. Box 1527, Heraklio, Crete, Greece 71110

Madhu Menon‡

Department of Physics and Astronomy and Center for Computational Sciences,

University of Kentucky, Lexington, KY 40506

Abstract

Using first principles calculations we demonstrate the existence of anisotropic ferromagnetic interactions in Co embedded graphene nanoribbons (GNR). Spin polarization of the edge states is found to alter significantly compared to the metal free cases. Our findings can all be well justified as the output of the interplay between the development of an induced spin polarization in the neighborhood of the Co atoms and the maintaining of the polarization picture of the Co-free GNR. Based on our results we propose an efficient pathway for graphene based spintronics applications.

PACS numbers: 75.75.-c,73.20.-r,75.50.Xx,75.70.Cn

*Electronic address: slisenk@cas.usf.edu

†Electronic address: andriot@iesl.forth.gr

‡Electronic address: super250@uky.edu

The experimental discovery of free standing graphene nanoribbons (GNRs)[1, 2] has generated renewed interest in pure carbon materials with exotic properties. GNR is essentially a single sheet of graphite confined by edges. These edges can be considered as defects in an otherwise infinite sp^2 network giving rise to many interesting electronic properties[3]. Depending on their edges, the GNRs can be classified either as zig-zag or of arm-chair type[4].

Even though pristine carbon materials are nonmagnetic, presence of defects has been used to explain the occurrence of magnetism in carbon based material[5–8]. These defects include dislocations, vacancies and impurity atoms. Graphene is one such carbon-based material that offers great promise for investigating unconventional magnetism in carbon-based materials. Of particular interest is the transition metal (TM) impurity induced magnetism in graphene that allows control of magnetic properties by controlling the TM contents. This is very useful in the context of spintronics applications for these materials.

There are two main avenues for incorporating TM atoms in graphene. One way is to have TM atoms adsorbed on graphene sheets. Although TM adatoms are known to bind strongly to graphene[9], the calculated migration barriers proved to be low enough for them to be mobile at room temperature[10]. This makes them unsuitable for use in graphene based devices operating at room temperatures and above. The second way is to incorporate TM atoms in graphene vacancies; single vacancy (SV) or double vacancy (DV). Very recently, the energetics as well as the structural and magnetic properties of individual TM atoms embedded in SV and DV in graphene have been studied[10–13]. The binding energies in these cases have been predicted to be far greater than those in the case of TM adatoms on graphene. Although both TM-SV and TM-DV complexes have been found to be magnetic, overall the TM-DV complex has been shown to generate larger magnetic moments[10]. It, therefore, appears that TM-DV complex offers the best avenue for graphene based magnetic devices.

In this Letter, supported by *ab initio* density functional theory (DFT) calculations, we present a systematic study of magnetic interactions between Co-DV complexes in graphene nano-ribbons (GNR) with a view to obtain optimal geometric configurations for ferromagnetic (FM) enhancement in these materials. The DFT calculations are performed in the spin polarized generalized gradient approximation (SGGA) of Perdew-Burke-Ernzerhof (PBE)[14] for exchange and correlation as implemented in the Vienna Ab-initio Simulation

Package (VASP)[15–17]. A Hubbard U term is added to the SGGA functional (SGGA+U) to model the Coulomb repulsion between $3d$ electrons localized on the Co atom. We assign the value U_d=2.0 eV based on our earlier calculations. This value has also been used for Co by other groups[9]. The projected augmented wave (PAW) potential[16, 17] is used to describe the core electrons. After testing for convergence we settled for a 8×1×1 Γ-centered pack for **k**-vectors sampling. A kinetic energy cutoff of 550 eV was found to be sufficient to achieve a total energy convergence of the energies of the systems to within 1 meV. Gaussian smearing of 0.05 eV was chosen to accelerate electronic convergence. The optimization of atomic positions (including full cell optimization) was allowed to proceed without any symmetry constraints until the force on each atom is less than 5 meV/Å.

The GNR supercells used in most of the simulations contained 160 atoms with additional calculations carried out for larger supercells containing 190 atoms for testing for convergence of the results. The effects of asymmetry on the FM stability was studied by shifting the Co-DV complex relative to the symmetry axis of the GNRs. Calculations of FM stability were also performed by varying the widths of GNRs. We have considered both bare as well as hydrogen saturated outer edges of the GNR supercells. No restriction on spin was imposed during the relaxation process. We take Co as a TM representative and construct the Co-DV complex by substituting a C-dimer in GNR with a single Co and relaxing the resulting structure. Co assumes a "cross" position in the plane of GNR while symmetrically bonded to the four C atoms with a bond length of 1.9 Å. The binding energy for Co in a substitutional DV position in GNR is calculated to be -4.5 eV. This is obtained by taking the energy difference between the Co in the substitutional position and the energy of the reconstructed bare vacancy plus the energy of the isolated Co atom. The binding for Co-DV is weaker than for Co-SV but still considerably stronger than the case when Co is an adatom on GNR[10].

In order to check the thermal stability of the Co-DV complexes, we performed *ab initio* molecular dynamics (MD) incorporating constant temperature MD simulations performed at 800 K using the Berendsen thermostat[18]. No dissociation of the structures were found indicating that the proposed complexes are thermally stable.

For studying a single Co-DV complex we have considered a 107 atom supercell. The Co-DV complex is found to be magnetic with the magnetic moment (MM) value on Co to be 1.82 Bohr Magneton (μ_B). This is similar to the value reported by other groups[10]. In

Fig. 1 we show a plot of magnetization values for this complex. The distribution of MMs show an interesting trend that can be better understood if the bipartite nature of graphene is recalled. In particular, the presence of Co interrupts the regular bipartite structure of the pristine graphene, transforming it into two separate bipartite structures, one above and one below the Co atom. As can be seen in Fig. 1, due to the influence of the Co atom, one of the pairs of the four nearest neighbor (nn) C atoms, namely the upper pair, become polarized with polarization direction opposite to that of Co. This pair, in turn, dictates the bipartite arrangement of magnetic moments of the upper part (above the Co-level). Similarly, the influence of the Co atom causes the lower pair of nn C atoms to polarize opposite to it and dictate the bipartite arrangement of magnetic moments of the lower part. The overall effect is to cause the lower edge of Fig. 1 to become spin polarized in the same direction (ferromagnetically aligned) as the upper edge.

We next study the magnetic interactions between two Co-DV complexes in GNR. We do this by first considering 160 atom supercells each containing 2 Co atoms. All edge C atoms are passivated by H. Each of the Co atom is located in a divacancy created by the removal of 2 C atoms. We only consider non-merging DV cases in which no direct Co-Co bonds are formed. A large number of configurations are considered in which the distances and the orientations of the Co-Co vectors are varied. In Fig. 2 we show a schematics summarizing our results. While each supercell has 160 atoms, only the relevant portions of the supercells are shown in Fig. 2 for clarity. The axis of the GNR is in the horizontal direction (towards right). The thick colored lines indicate the bonds between 2 C atoms that were removed to create the DV. The location of the Co atom is in the center of the thick colored lines. FM interaction is indicated by the green lines while the antiferromagnetic (AFM) interaction is indicated by the red.

A number of very interesting features can be observed in Fig. 2 with the most intriguing being the anisotropy of the magnetic interactions. Specifically, if a two dimensional cone is visualized with its tip at one of the Co atoms with its axis along the axis of the GNR (see the blue inset in Fig. 2), then according to the results shown in Fig. 2, FM interaction ensues if the second Co atom is located within a cone of an angle of about 100 degrees. The interaction changes to AFM when the second Co atom is outside this cone. The observed anisotropy appears to be the result of the interplay between the Co-induced and the edge-induced spin polarization in combination with the bipartite structure of the graphene as

discussed in the above. Thus, enhanced FM (AFM) is found for DVs along (perpendicular to) the graphene axis, respectively.

In Table I we list the relative energies and the energy differences between FM and AFM states, ΔE=E$_{FM}$-E$_{AFM}$, of all configurations in Fig. 2 as well as the MMs of the two Co atoms in each case. The lowest energy configuration is found to be the complex c which is one of the closest non-merging Co-DV cases. This is followed by other close non-merging Co-DV configurations e and j. An interesting trend can be seen in configurations a, b and i where the Co-DVs are aligned along the GNR axis. Although the relative energies increase (becoming less stable) as the separation between the Co-DVs increase, the E$_{FM}$-E$_{AFM}$ difference (FM strength), is also found to increase. A reverse trend is seen for the AFM cases in d and h where increased separation leads to increased stability but decreased AFM strength. The closest non-merging Co-DV configuration g is also the most stable among the AFM configurations. Examining the results of our calculations by shifting the Co-DV complex relative to the symmetry axis of the GNR to simulate asymmetry, we find that asymmetry significantly enhances the ferromagnetic stability (i.e., the E$_{FM}$-E$_{AFM}$ difference) for both i and k configurations. Increasing the GNR width, on the other hand leads to a decrease in the FM stability.

In Fig. 3 we show a plot of magnetization values for the lowest energy Co-DV complex c in Fig. 2. As in the Co-SV case, the total MM of the system comes mostly from the Co atoms with some spin polarization for the C atoms. In order for a better understanding of the development of MMs in the GNR as a result of Co incorporation, we performed calculations for the band structure and density of states (DOS) for all the Co-DV complexes shown in Fig. 2. The results are plotted in Fig. 4 for the Co-DV complex c in Fig. 3. As seen in the figure, there are a number of strongly hybridized states of Co-d and C-p character that appear at and below the Fermi energy, E$_F$ exhibiting spin-polarization for the Co atoms as well as their nearest neighbor C atoms.

Our findings allow us to arrive at some significant conclusions. In particular, as can be seen from Fig. 3, the Co-cations induce magnetic MMs on their nn C atoms which are aligned anti-parallely with respect to the MM of the inducing Co atom. This has a dramatic effect on the distribution of spins on the rest of the C-atoms as it breaks the symmetry of the bipartite structure. Specifically, as mentioned in the above, we find that the C atoms which are 1st nn to a Co atom, specify the MMs on the whole zig-zag C-lines running parallel to

GNR-axis on which they are located. The rest of the zig-zag C-lines (also running parallel to the GNR axis) then exhibit an alternative sequence of MM alignments leading up to the GNR-edges, which contrary to the Co-free GNR case, can be FM coupled. The presence of the second Co atom (Co2) enhances this picture as shown, for example, in Fig. 3. In particular, the C atoms that are nn to Co1, while maintaining their polarization direction dictated by the presence of Co1, make it energetically favorable for Co2 to be oppositely polarized to them. This, in turn, causes the C atoms that lie on the opposite side of Co2 to have their MMs specified by it. These results show that the polarization pattern of the edge atoms of the GNR is determined by the position of the Co atoms and the level of the spin frustration that is introduced by breaking the bipartite structure. It should be noted that the Co-free graphene exhibits spin polarized edge states with opposite polarization as a result of a superexchange interaction[19–21]. These edge states decay towards the central axis of the GNR with an oscillating amplitude. As shown by us, this picture seems to be drastically altered by the presence of the Co atoms. Our calculations indicate that the disturbance depends on the defect configuration and the overall spin configuration appears to be an interplay between the development of an induced spin polarization in the neighborhood of the Co atoms and the maintaining of the polarization picture of the Co-free GNR (i.e., an alternate polarization along a line perpendicular to the central axis). The outcome of this interplay is thus a measure of how well the impurity-defect complexes fit into the bipartite structure of graphene.

Additionally, the same arguments can be used to justify why in the defect configurations a, i and b, the FM coupling increases as the distance between the Co atoms increases. This can be attributed to the fact that an increase in the distance between the Co atoms results in the enhancement of the length of the zig-zag line (on which the 1st nn C-atoms are located) over which we have an enhancement of the induced MMs.

For Co in DV, its d orbitals split into two orbital doublets of E symmetry and a singlet of A1 symmetry[22, 23]. The spin 1.5 of Co consists of spin 1 from its $3d$ orbital of E symmetry which is ferromagnetically coupled to a spin 1/2, mainly from its $4s$ orbital. Our analysis reveals that Co loses 1.5 electrons from its d, and s orbitals on hybridization with the graphene DV states. The 1.5 spin of Co can then be justified by considering that Co gives up a spin-down electron and 1/2 of a spin-up electron, both from its $4s$ orbital.

In conclusion, using *ab initio* calculations we demonstrated the anisotropy of magnetic

interactions in Co embedded GNRs. Our findings, presented in Fig. 2, can all be well justified on the basis of a mutually synergistic spin-polarization the Co atoms induce on their nn C-atoms. Our results indicate that placing of the Co atoms can be used to favor the FM alignment as well as to engineer the magnetic behavior of the edges of the ribbons thus providing a significant tool for device applications.

Very recently experimentalists have succeeded in using an electron beam to bore holes into single and double layers of graphene[24]. The TM-DV complex can then be created by pinning TM atoms on vacancies created this way using a mechanism proposed recently[10, 12]. Recent experiments have confirmed observation of substitutional TM atoms in graphene[25]. Furthermore, the large activation energies for in-pane migration observed in the experiment point toward strong covalent carbon-metal bonding and high stability for such defects.

The present work is supported through grants by DOE (DE-FG02-00ER45817 and DE-FG02-07ER46375).

[1] J. C. Meyer, A. K. Geim, K. S. Novoselov, T. J. Booth, and S. Roth, Nature **446**, 60 (2007).

[2] S. V. Morozov, K. S. Novoselov, M. I. Katsnelson, F. Schedin, L. A. Ponomarenko, D. Jiang, and A. K. Geim, Phys. Rev. Lett. **97**, 016801 (2006).

[3] K. Nakada, M. Fujita, G. Dresselhaus, and M. S. Dresselhaus, Phys. Rev. B **54**, 17954 (1996).

[4] An infinite (straight) graphene ribbon is characterized as arm-chair type or zig-zag type if its edges parallel to its axis exhibit the arm-chair or the zig-zag structure. This terminology is followed for the finite GNRs as well.

[5] T. L. Makarova, B. Sundquist, R. Hohne, P. Esqulnazi, Y. Kopelevich, P. Scharff, V. A. Davidov, L. S. Kashevarova, and A. V. Rakhmanlna, Nature **413**, 716 (2001).

[6] A. N. Andriotis, M. Menon, R. M. Sheetz, and L. Chernozatonskii, Phys. Rev. Lett **90**, 026801 (2003).

[7] P. O. Lehtinen, A. S. Foster, Y. Ma, A. V. Krasheninnikov, and R. M. Nieminen, Phys. Rev. Lett. **93**, 187202 (2004).

[8] S. Lisenkov, A. N. Andriotis, and M. Menon, Phys. Rev. B **82**, 165454 (2010).

[9] K. T. Chan, H. Lee, and M. L. Cohen, Phys. Rev. B **83**, 035405 (2011).

[10] A. V. Krasheninnikov, P. O. Lehtinen, A. S. Foster, P. Pyykko, and R. M. Nieminen, Phys. Rev. Lett. **102**, 126807 (2009).

[11] D. W. Boukhvalov and M. I. Katsnelson, Appl. Phys. Lett. **95**, 023109 (2009).

[12] E. J. G. Santos, D. Sanchez-Portal, and A. Ayuela, Phys. Rev. B **81**, 125433 (2010).

[13] V. V. Nelayev and A. I. Mironchik, Mater. Phys. Mech. **9**, 26 (2010).

[14] J. P. Perdew, K. Burke, and M. Ernzerhof, Phys. Rev. Lett. **77**, 3865 (1996).

[15] G. Kresse and J. Hafner, Phys. Rev. B **47**, 558 (1993).

[16] G. Kresse and D. Joubert, Phys. Rev. B **59**, 1758 (1999).

[17] P. E. Blochl, Phys. Rev. B **50**, 17953 (1994).

[18] H. J. C. Berendsen, J. P. M. Postma, W. F. van Gunsteren, A. DiNola, and J. R. Haak, J. Chem. Phys. **81**, 3684 (1984).

[19] M.Fujita, K.Wakabayashi, K.Nakada, and K.Kusakabe, J.Phys.Soc. Japan, 65, 1920 **65**, 1920 (1996).

[20] J. Jung, T. Pereg-Barnea, and A. H. MacDonald, Phys. Rev. Lett. **102**, 227205 (2009).

[21] O. V. Yazyev, R. B. Capaz, and S. G. Louie, Phys. Rev. B **84**, 115406 (2011), URL http://link.aps.org/doi/10.1103/PhysRevB.84.115406.

[22] K. T. Chan, H. Lee, and M. L. Cohen, Phys. Rev. B **83**, 035405 (2011), URL http://link.aps.org/doi/10.1103/PhysRevB.83.035405.

[23] T. O. Wehling, A. V. Balatsky, M. I. Katsnelson, A. I. Lichtenstein, and A. Rosch, Phys. Rev. B **81**, 115427 (2010), URL http://link.aps.org/doi/10.1103/PhysRevB.81.115427.

[24] S. Garaj, W. Hubbard, A. Reina, J. Kong, D. Branton, and J. A. Golovchenko, Nature **467**, 190 (2010).

[25] Y. Gan, L. Sun, and F. Banhart, Small **4**, 587 (2008).

Configuration	Magnetic state	Relative energy eV/cell	ΔE =E$_{FM}$-E$_{AFM}$ eV/cell	Magnetic moment (μ_B)	
				Co1	Co2
a	FM	0.673	-0.019	1.592	1.610
b	FM:	1.226	-0.204	1.725	1.725
c	FM	0.000	-0.142	1.713	1.629
d	AFM	1.405	0.720	-1.744	1.809
e	FM	0.231	-0.012	1.751	1.095
f	FM	0.574	-0.052	1.420	1.574
g	AFM	0.852	0.076	-1.632	1.879
h	AFM	0.713	0.110	-1.820	1.899
i	FM	0.926	-0.109	1.494	1.485
j	FM	0.353	-0.168	1.830	1.837
k	FM	0.688	-0.123	1.496	1.518

TABLE I: Relative energies (with respect to the ground state) and magnetic moments (for Co1 and Co2) of various configurations shown in Fig. 2.

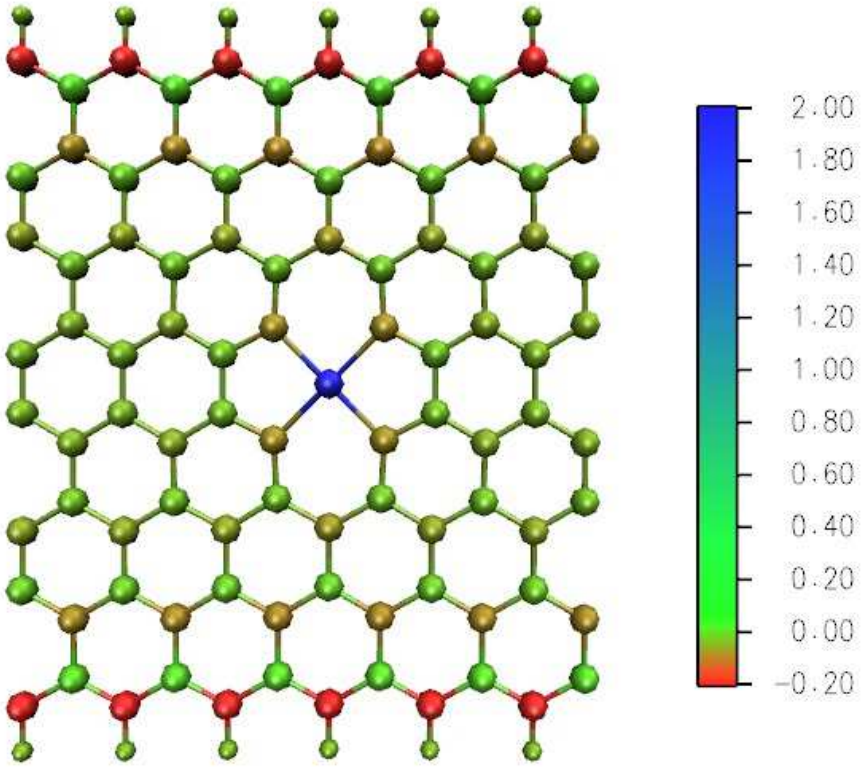

FIG. 1: Figure showing the magnetic moments of Co-DV complex in GNR. The GNR is periodic in the x-direction. The dangling bonds on the bare edge C atoms have been saturated with H.

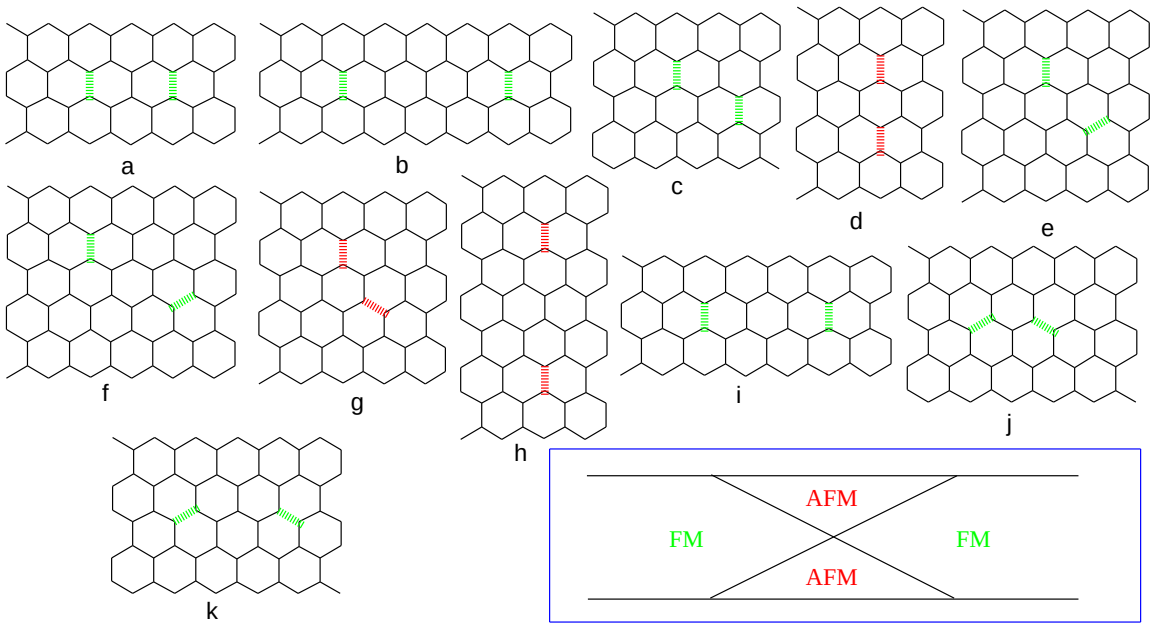

FIG. 2: Schematics showing various Co-DV complexes considered. Even though each supercell has 160 atoms, only the relevant portions of the supercells are shown for clarity. The axis of the GNR is in the horizontal direction. The thick colored lines indicate the bonds between 2 C atoms that were removed to create the DV. The location of the Co atom is in the center of the thick colored lines. FM interaction is indicated by the green lines while AFM is indicated by the red. The two dimensional cone separating FM and AFM interactions is shown in the blue inset.

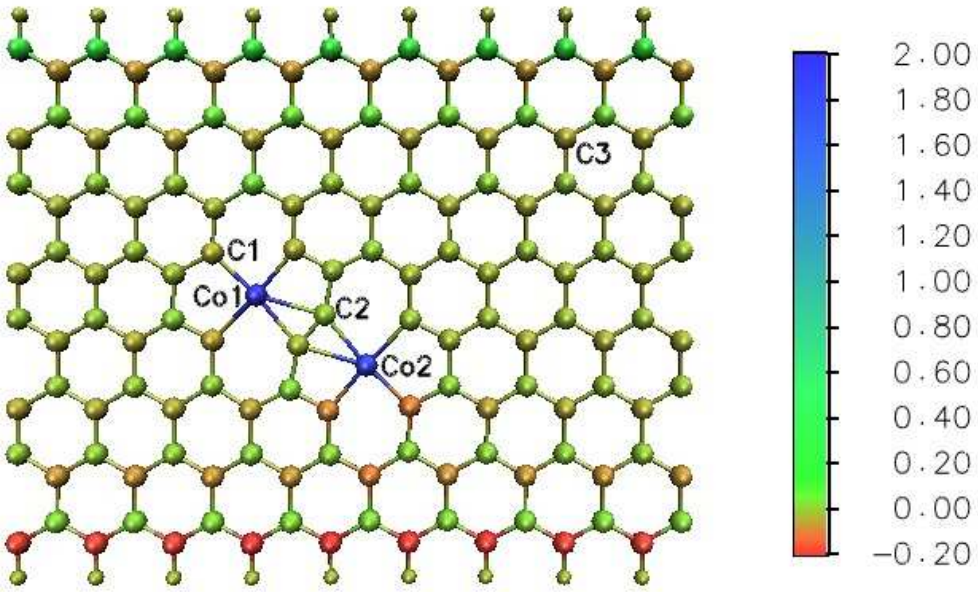

FIG. 3: Figure showing the magnetic moments of the lowest energy Co-DV pair complex configuration c of Fig. 2.

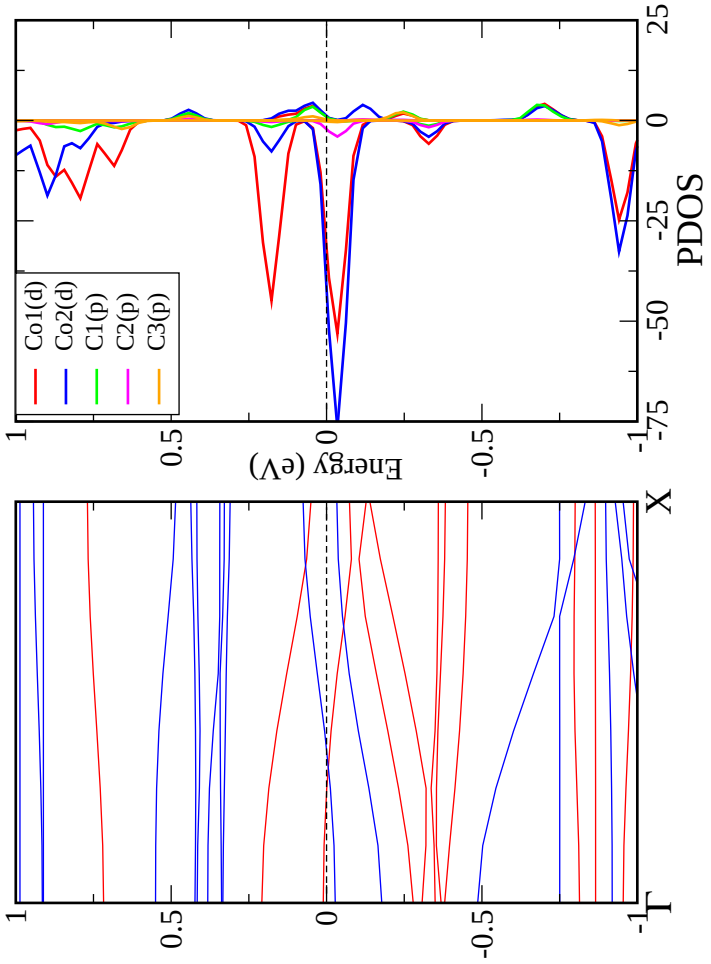

FIG. 4: Band structure and spin-polarized DOS of the lowest energy Co-DV pair complex complex c in Fig. 3. In the figure on the left, red (blue) lines represent the majority (minority) spins. The Fermi energy is at zero. In the figure on the right, positive/negative DOSs denote majority/minority spin-DOSs, respectively.